DOI: 10.1534/genetics.110.120519

Genetics of Extracellular Matrix Remodeling During Organ Growth Using the *Caenorhabditis elegans* Pharynx Model

Gholamali Jafari,* Jan Burghoorn,† Takehiro Kawano,‡,§ Manoj Mathew,*, Catarina Mörck,*,[1] Claes Axäng,* Michael Ailion,††,[2] James H. Thomas,†† Joseph G. Culotti,‡ Peter Swoboda† and Marc Pilon*,[3]**

**Department of Cell and Molecular Biology, University of Gothenburg, S-405 30 Gothenburg, Sweden, †Department of Biosciences and Nutrition, Karolinska Institute, Center for Biosciences at NOVUM, S-141 83 Huddinge, Sweden, ‡Samuel Lunenfeld Research Institute of Mount Sinai Hospital, Toronto M5G 1X5, Canada, §Department of Molecular Genetics, University of Toronto, Toronto M5S 1A8, Canada, **Institut de Ciències Fotòniques, 08860 Castelldefels (Barcelona), Spain and ††Department of Genome Sciences, University of Washington, Seattle, Washington 98195*

Manuscript received July 2, 2010
Accepted for publication August 25, 2010

ABSTRACT

The organs of animal embryos are typically covered with an extracellular matrix (ECM) that must be carefully remodeled as these organs enlarge during post-embryonic growth; otherwise, their shape and functions may be compromised. We previously described the ***twi***sting of the *Caenorhabditis elegans* ***p***harynx (here called the Twp phenotype) as a quantitative mutant phenotype that worsens as that organ enlarges during growth. Mutations previously known to cause pharyngeal twist affect membrane proteins with large extracellular domains (DIG-1 and SAX-7), as well as a *C. elegans* septin (UNC-61). Here we show that two novel alleles of the *C. elegans* papilin gene, *mig-6(et4)* and *mig-6(sa580)*, can also cause the Twp phenotype. We also show that overexpression of the ADAMTS protease gene *mig-17* can suppress the pharyngeal twist in *mig-6* mutants and identify several alleles of other ECM-related genes that can cause or influence the Twp phenotype, including alleles of fibulin (*fbl-1*), perlecan (*unc-52*), collagens (*cle-1*, *dpy-7*), laminins (*lam-1*, *lam-3*), one ADAM protease (*sup-17*), and one ADAMTS protease (*adt-1*). The Twp phenotype in *C. elegans* is easily monitored using light microscopy, is quantitative via measurements of the torsion angle, and reveals that ECM components, metalloproteinases, and ECM attachment molecules are important for this organ to retain its correct shape during post-embryonic growth. The Twp phenotype is therefore a promising experimental system to study ECM remodeling and diseases.

EVERY tissue and organ of multicellular animals is surrounded by a specialized extracellular matrix (ECM) that supports their shapes and mechanical properties and contributes adhesive substrates while coordinating the sequestering and availability of guidance cues and growth factors during development (Rozario and Desimone 2010; Tsang *et al.* 2010). The composition of the ECM varies with the needs of the tissues and organs, but typically includes networks of collagen, laminin, or fibronectin, which are interconnected by molecules such as fibulin and the proteoglycans perlecan and nidogen.

Organs usually complete their basic assembly during embryogenesis and later development mostly consists of the enlargement of these organs. This must be accompanied by remodeling of the ECM that surrounds the organs and tissues, a phenomenon that is further complicated by allometry, *i.e.*, the fact that different organs grow at different rates, and by the varying mechanical requirements of the different organs. There are dozens of human genetic disorders where defects in ECM remodeling during growth are the likely causes of disease (Carter and Raggio 2009). Unfortunately, except for the Drosophila tracheal system, there are few established genetic models to study ECM remodeling during organ growth. In Drosophila, the regulation of a luminal ECM matrix containing chitin determines tracheal tube diameter (Tonning *et al.* 2005; Laprise *et al.* 2010), and matrix metalloproteinases that can degrade ECM components are essential for the growth-related remodeling of the tracheal tubes themselves (Glasheen *et al.* 2010).

The *Caenorhabditis elegans* pharynx is a straight feeding tube responsible for rhythmically pumping, trapping, and grinding bacterial food before passing it on to the intestine (Albertson and Thomson 1976; Avery and Shtonda 2003). The pharynx, which is surrounded

Supporting information is available online at http://www.genetics.org/cgi/content/full/genetics.110.120519/DC1.

[1]*Present address:* Department of Molecular and Cell Biology, University of California, Berkeley, CA 94720.

[2]*Present address:* Department of Biology, University of Utah, 257 S. 1400 East, Salt Lake City, UT 84112-0840.

[3]*Corresponding author:* Department of Cell and Molecular Biology, University of Gothenburg, Medicinaregatan 9C, S-405 30 Göteborg, Sweden. E-mail: marc.pilon@cmb.gu.se

by a thick basement membrane (C. C. Huang *et al.* 2003; Kramer 2005), is composed of 80 cells (some fuse post-embryonically to produce an organ with 63 cells but 80 nuclei) and exhibits threefold symmetry, with one dorsal and two subventral muscular sectors containing radially directed contractile arrays. It is attached to the mouth via hemidesmosomes between pharyngeal epithelial cells and the arcade cells of the mouth and to the intestine via the pharyngeal-intestinal valve composed of six cells (Albertson and Thomson 1976). Four rows of 12–15 tendons composed of hemicentin and fibulin also secure the anterior part of the pharynx to the body wall of the worm (Vogel and Hedgecock 2001; Muriel *et al.* 2005). The pharynx develops during embryogenesis from a semispherical primordium that elongates as cells differentiate to form the mature elongated structure (Portereiko and Mango 2001), and this process is under the control of the forkhead transcription factor PHA-4 that seems to regulate most pharyngeal genes (Mango *et al.* 1994; Horner *et al.* 1998; Kalb *et al.* 1998; Gaudet and Mango 2002).

We previously described the twisted pharynx (Twp) phenotype as being easily monitored and quantifiable by DIC microscopy (Axäng *et al.* 2007). Mutants with the Twp phenotype have fully functional pharynges with normal pumping rates. The twisted phenotype itself is likely growth-related: the pharyngeal twist becomes visible post-embryonically, worsens as the organ enlarges during post-embryonic growth, is not enhanced by pharyngeal pumping in the absence of food or once adult size is reached, and affects more severely the parts of the pharynx that are thinner, while mutants with a thickened pharynx show less twist (Axäng *et al.* 2007). In a survey of candidate mutants, we identified alleles in four genes that could cause the Twp phenotype: *unc-61*, which encodes a septin (Nguyen *et al.* 2000); *dig-1* and *sax-7*, which encode transmembrane proteins with very large extracellular domains (Sasakura *et al.* 2005; Wang *et al.* 2005; Bénard *et al.* 2006; Burket *et al.* 2006); and *mig-4*, which affects a hitherto unidentified gene. Another mutant allele, *mnm-4(et4)*, was isolated in a forward genetics screen for abnormal pharynges and also remained unidentified (Axäng *et al.* 2007). Here we show that *et4* and the noncomplementing allele *sa580* are actually novel alleles of *mig-6*, which encodes the *C. elegans* homolog of papilin, a component of the ECM that contains several domains homologous to ADAMTS-like proteins. We also identify genes for collagen XVIII (*cle-1*), cuticle collagen (*dpy-7*), fibulin, laminin, perlecan, and metalloproteinases as participating in ECM remodeling during organ growth.

MATERIALS AND METHODS

Strains and *C. elegans* maintenance: The wild-type *C. elegans* strain used in this project was Bristol N2 (Brenner 1974; Sulston and Hodgkin 1988). *C. elegans* worms were maintained at 20° using standard methods (Sulston and Hodgkin 1988). All *C. elegans* strains were obtained from the *C. elegans* Genetics Center in Minneapolis, Minnesota (http://www.cbs.umn.edu/CGC/), except for strains containing the following previously described alleles of *mig-6* (Kawano *et al.* 2009): *ev700*, *ev701*, *ev788*, *e1931*, *k177*, and *oz113*. The *mig-6(sa580)* allele was isolated in a screen for high-temperature dauer formation, where all candidate mutant animals were also cross-examined for anatomical defects of the amphid neurons (Ailion and Thomas 2003). Later analysis showed that *sa580* was a background mutation and does not itself have a dauer phenotype. The *mig-6(et4)* allele was isolated in a screen for abnormal pharyngeal neurons (Mörck *et al.* 2003).

Nomarski (DIC) microscopy and scoring of the Twp phenotype: Animals were placed on 2% agarose pads (0.04 g agarose, 2 ml 0.05% phenoxypropanol) on glass slides in a drop of 0.02% phenoxypropanol as anesthetic and overlaid with a cover slip. Animals were observed with a Zeiss Axiophot microscope using a GFP filter or Nomarski optics. Images were taken using the Axiovision 4.5 program (Zeiss) and further processed using Photoshop (Adobe). To measure the torsion angle, L4 larvae were picked and 24 hr later the pharynx of each young adult was photographed under Nomarski optics on a focal plane that showed the strongest twist within the upper half of the worm. The angle formed by the torsion lines in each twisted pharynx was measured twice using the public domain software ImageJ (National Institutes of Health) and the mean was recorded as one entry. In cases where there was obviously no twist as determined by microscopic examination, the pharynx was scored as having a torsion angle of 0° without recourse to ImageJ. In Tables 1–3, the minimum and maximum torsion angles observed for each genotype scored are provided, together with the mean ± SEM of the torsion angles of all the worms photographed and the fraction of twisted pharynges that twisted to the left.

Second harmonic generation microscopy: Second harmonic generation (SHG) microscopy was performed on pharyngeal muscles using a specially adapted confocal microscope (Mathew *et al.* 2009) that facilitates nonlinear microscopy. Light with a wavelength of 868 nm from a tuneable, 160-fsec pulse duration, 76-MHz repetition rate ultrashort pulsed laser (Coherent MIRA 900f) was employed. The laser beam with 15–18 mW average power (on the sample plane) was scanned across the sample. The SHG signal was collected using an oil immersion condenser with a high numerical aperture (1.4) and detected using a photo multiplier tube that accommodates a 434-nm (half of 868 nm) narrow band pass optical filter. The SHG signal is produced intrinsically in ordered structures such as muscle, and the SHG signal detected during the laser scanning process is converted to an image exactly as with a confocal microscope.

Fluorescent dye-filling assay: 1,1'-dioctadecyl-3,3,3'3'-tetramethylindocarbocyanine perchlorate (DiI) preferentially fills some amphid head neurons and phasmid tail neurons (Perkins *et al.* 1986; Starich *et al.* 1995). Stock solutions of the fluorescent Vybrant DiI cell-labeling solution (Invitrogen) were stored at −20°, and DiI dye-filling assays were performed by incubating worms for 2 hr at 20° in 10 mg/ml of DiI in M9 buffer solution. After incubation, the animals were washed three times with M9 and observed using a fluorescence microscope (Axiophot, Zeiss).

Plasmid constructs: pZH125 and pZH117 carry *mig-6S* and *mig-6L* minigenes, respectively, and have been described previously (Kawano *et al.* 2009). The pQC10.1 and pQC10.2 plasmids were derived from pZH125 and carry *mig-6S* minigenes with the *mig-6(et4)* and *mig-6(sa580)* mutations, respectively. A fragment of 1540 bp spanning parts of *mig-6* exons 8 and 9 was amplified from genomic DNA of *mig-6(et4)* or *mig-*

6(sa580) mutant worms using Pfu Ultra DNA polymerase and the following primers: *Pst*I_mig-6 F (5′-ctgcagcgtcacaaacgag-3′) and *Pst*I_mig-6 R (5′-ctgcagatgtcttccattg-3′). The PCR product was subcloned into pCR_Blunt_II_TOPO (Invitrogen), and the resulting construct was cut with *Pst*I. The released 1540-bp fragment was subcloned into the *Pst*I site of pZH125 to generate pQC10.1 or pQC10.2. Restriction enzyme mapping and sequencing confirmed the correct orientation and structure. The *mig-17::GFP* fusion construct was a kind gift from K. Nishiwaki (Nishiwaki *et al.* 2000).

Transgenic worms: Where applicable, 20 ng/μl of pZH125, pZH117, pQC10.1, and pQC10.2 were coinjected into the gonad syncytium of adult hermaphrodites (Mello *et al.* 1991) with 48 ng/μl of *pCC::gfp*, a coelomocyte transformation marker (Miyabayashi *et al.* 1999), and transgenic worms were identified by their GFP-positive coelomocytes.

RNA interference: RNA interference (RNAi) by feeding was done using a published RNAi library and as previously described (Kamath *et al.* 2001). The following genes, with the open reading frame name given in parentheses, were knocked down by RNAi: *adm-2* (C04A11.4), *adt-1* (C02B4.1), *agr-1* (F41G3.12), *cle-1* (C36B1.1), *dgn-1* (T21B6.1), *dpy-7* (F46C8.6), *emb-9* (K04H4.1), *epi-1* (K08C7.3), *fbl-1* (F56H11.1), *gon-1* (F25H8.3), *lam-1* (W03F8.5), *lam-3* (T22A3.8), *let-2* (F01G12.5), *mig-6* (C37C3.6), *mig-17* (F57B7.4), *mig-23* (R07E4.4), *sup-17* (DY3.7), *unc-22* (ZK617.1), *unc-52* (ZC101.2), and *unc-71* (Y37D8A.13). For each of the genes of interest, two plates were seeded with 500 μl liquid bacteria and then allowed to dry overnight at 20°. The following day, four L3 stage hermaphrodite worms were transferred onto the first plate containing seeded bacteria expressing double-stranded RNA and incubated for 72 hr at 20°. Then, L4 animals (F_1) were transferred onto the second plate, seeded with the same bacterial clone, and incubated for 24 hr at 20°. Young adults were then microscopically examined to analyze the RNAi effects. *unc-22* was used as a positive control for the RNAi method and always produced a typical twitching phenotype. For the RNAi experiments, IPTG (1 mm) and carbenicillin (25 μg/ml) were added to the NGM agar worm plates, and tetracycline (12.5 μg/ml) was included in the bacterial liquid cultures to maintain the RNAse-deficient clones.

RESULTS

The pharyngeal twist (Twp) phenotype: We previously characterized the Twp phenotype and described a method to quantify the degree of twist using the equation:

$$\text{Twist}^\circ = (L \tan\theta)/D\,\pi \times 360^\circ.$$

The equation is based on the measurements of the isthmus length (L), diameter (D), and torsion angle θ formed between the torsion lines and the pharyngeal longitudinal axis (Axäng *et al.* 2007). In age-matched worms of similar pharynx sizes, it is more expedient to quantify the Twp phenotype by measuring only the torsion angle θ. In our earlier report, we also described the *et4* mutant allele and showed that it exhibits a post-embryonic pharyngeal left-handed Twp phenotype that worsens during larval growth (Axäng *et al.* 2007). The pharyngeal twist is easily imaged using Nomarski optics (Figure 1, A–D), and the torsion angle θ is highly reproducible among age-matched animals; for example, *et4* homozygous animals have a torsion angle of 28.9° ± 1.2°. Imaging of wild-type and twisted pharynges using SHG microscopy, which is a high-resolution and dye-independent method to generate three-dimensional images of noncentrosymmetric quasi-crystalline structures, such as are formed by the contractile arrays within muscle cells (Psilodimitrakopoulos *et al.* 2009), shows that the pharyngeal muscles are also twisted but not grossly compromised in their subcellular architecture (Figure 1, E and F). This is consistent with the observation that *et4* mutants are not feeding-defective and exhibit perfectly normal pharyngeal contraction cycles (Axäng *et al.* 2007).

An obvious question is whether other structures in addition to the pharynx are twisted within the head in *et4* mutant worms. We addressed this by visualizing the dendrites of amphid neurons that run along the side of the pharynx and terminate around the mouth. Amphid neurons can be visualized using the fluorescent dye DiI (Perkins *et al.* 1986; Starich *et al.* 1995). In wild-type worms, the DiI-filled amphid neurons run straight along the pharynx surface in 100% of the animals (Figure 1, G and H). In *et4* mutants, we noted that, while 100% of the animals have the Twp phenotype, the amphid neurons are either straight (75% of cases) or conspicuously twisted (25% of cases) ($n = 20$; Figure 1, I–L). This result suggests that the degree of adhesion between amphid neuron dendrites and the pharynx is variable and that strong adhesions may cause the amphid dendrites to twist together with the pharynx during growth. The twist is likely an intrinsic property of the pharynx in *et4* mutant animals, and any twisting of extrapharyngeal structures is likely a secondary consequence.

The *et4* and *sa580* mutations are novel alleles of *mig-6*: The *et4* allele is semidominant (Axäng *et al.* 2007). A second allele of the same locus, *sa580*, came to our attention during the course of this study (*cf.* materials and methods) (Ailion and Thomas 2003) and, upon characterization, turned out to be slightly less semidominant than *et4*: while heterozygotes of *et4* exhibit an average torsion angle of 14° ± 1.2°, *sa580* heterozygotes have an average angle of 8.3° ± 1.1°. Doubly heterozygous animals have average twist angles of 21.9° ± 1.1°, consistent with noncomplementation of the two alleles. As with the *et4* allele, only the pharynx and a fraction of the amphid neurons embedded in the pharyngeal ECM are twisted in *sa580* mutant animals. For example, while pharyngeal muscles and neurons are clearly twisted, body neurons and amphid socket cells are not (supporting information, Figure S1).

By genetic mapping using recombinants between visible genetic markers and then between single nucleotide polymorphisms that distinguish the parental N2 strain from the Hawaiian strain CB4856, we defined the position of the *et4* and *sa580* mutations to a narrow

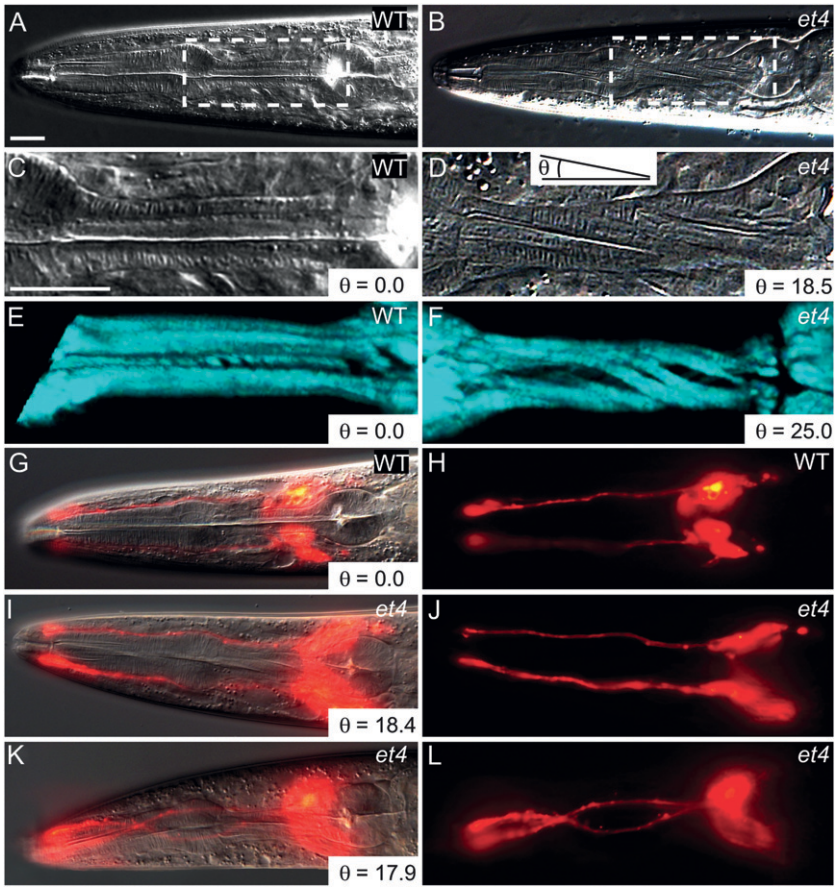

FIGURE 1.—The Twp phenotype in the *mig-6(et4)* mutant. (A) The head of a wild-type animal, with the boxed area enlarged in C. Note that the pharyngeal structures are perfectly straight along the anterior–posterior axis. (B) The head of a *mig-6(et4)* mutant, with the boxed area enlarged in D. Note the torsion lines indicative of a twisted pharynx. The angle θ is defined here as that formed by the torsion lines of the muscles and the anterior–posterior axis, as shown in D. (E and F) A wild-type and *mig-6(et4)* mutant pharynx, respectively, imaged using SHG microscopy at successive focal planes and rendered three dimensionally. Note the twisted appearance of the muscles in the mutant. A wild-type worm stained with DiI is shown as an overlay of DIC and epifluorescence in G or epifluorescence only in H. Note that the DiI-filled amphid neurons are straight. (I–L) *mig-6(et4)* mutants similarly stained with DiI, with DIC and epifluorescence overlays in I and K and epifluorescence only in J and L. Note that one worm displays straight amphid neurons (I and J) while the other has twisted amphid neurons (K and L), even though both have twisted pharynges as indicated by the angle θ in I and K. Bars, 20 μm, with the bar in panel C applying to panels C through F, and the bar in panel A applying to all other panels.

region of chromosome V (Figure 2A). We then tested six cosmids for their ability to rescue the Twp phenotype (Table 1 and Figure 2A). Two cosmids, ZK742 and C37C3, scored positive in this assay but only when co-introduced. Upon examination of the sequences, we noted the presence of the *mig-6* gene at the left end of the C37C3 cosmid, with the upstream regulatory 5′ region lying within cosmid ZK742 (Figure 2, A and B). Genomic DNA covering the *mig-6* locus was amplified from *et4* and *sa580* mutants, and sequencing revealed the presence of single point mutations: the *et4* allele carries a G-to-A transition that changes a cysteine at position 973 to a tyrosine, and *sa580* carries a G-to-A transition that changes a glycine at position 965 to a glutamate (Figure 2, C and D). The *et4* and *sa580* alleles are therefore novel variants of the *mig-6* gene and will be referred to as *mig-6(et4)* and *mig-6(sa580)*.

The *mig-6* mRNA can be spliced in alternative ways to produce a short protein, MIG-6S, and a long protein, MIG-6L (Figure 2, C and D) (KAWANO *et al.* 2009). Introduction of either the *mig-6S* or the *mig-6L* minigenes rescued the twisted pharynx in both the *et4* and *sa580* mutants (Table 1 and Figure 3). Conversely, introduction into wild-type worms of mutant forms of the *mig-6* minigene, harboring either the *et4* or the *sa580* mutation, caused the left-handed Twp phenotype (Table 1 and Figure 3). The ability of the mutant minigenes to cause Twp is consistent with the fact that both alleles are semidominant.

The MIG-6 proteins are homologous to the Drosophila protein Papilin and the *Manduca sexta* protein lacunin (NARDI *et al.* 1999) and include a domain structure similar to the ancillary domains of ADAMTS metalloproteinases (Figure 2D). In Drosophila, Papilin is abundantly present in most ECM and is essential for development (CAMPBELL *et al.* 1987; KRAMEROVA *et al.* 2000, 2003; FESSLER *et al.* 2004). In *C. elegans*, MIG-6S and MIG-6L are secreted proteins that contribute to the ECM and genetically interact with the ADAMTS protease MIG-17 and with collagen IV (KAWANO *et al.* 2009). Interestingly, none of six other alleles of *mig-6* that we tested showed the Twp phenotype (Table 1), although all do display typical defects in distal tip cell migration during gonad development either during the longitudinal phase of distal tip cell migration (class *-l* alleles) or during the second migration phase (class *-s* alleles) (KAWANO *et al.* 2009). The *mig-6(et4)* and *mig-6(sa580)* alleles have by themselves no defects in distal tip cell migration and therefore represent a novel allele class, *i.e.*, class *-twp*. These results uncouple the pharyngeal and gonad phenotypes and suggest the possibility of a pharynx-specific function for the eighth lagrin repeat (NARDI

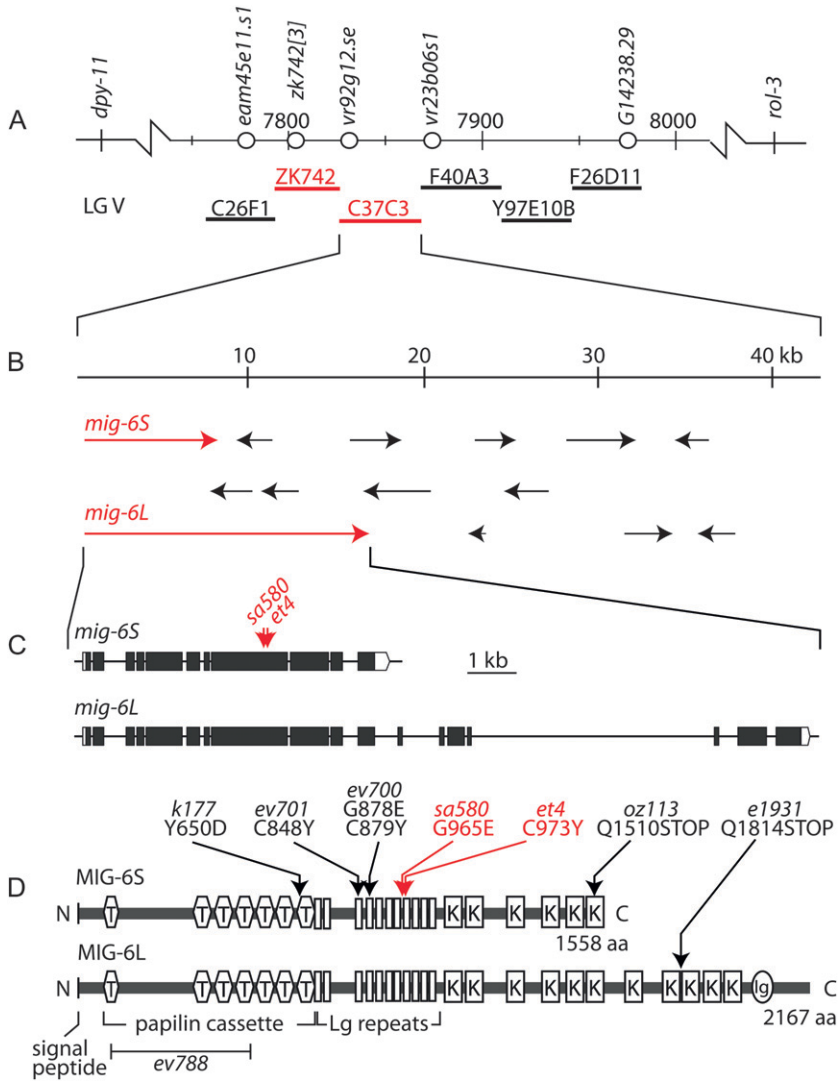

FIGURE 2.—Mapping of the *mig-6(et4)* and *mig-6(sa580)* mutant alleles. (A) Part of the map for chromosome V, including the positions of the genetic markers used to map *et4* and *sa580*. Single nucleotide polymorphisms that distinguish the wild-type N2 genome from the Hawaiian strain CB4856 are shown as open circles and the numbered positions refer to chromosomal locations expressed in kilobases. The locations of six cosmids that were tested for their ability to rescue the *sa580* mutant are also shown (thick horizontal lines). The ZK742 and C37C3 cosmids could rescue the *sa580* pharynx only when co-injected. (B) Enlarged view of the cosmid C37C3 showing genes as arrows and the two variants of the *mig-6* gene in red. (C) Structure of the *mig-6* gene showing the positions of the *et4* and *sa580* mutant alleles, which are both G-to-A transitions. (D) Domain structure of the MIG-6S and MIG-6L proteins, with the *et4* and *sa580* amino acid substitutions indicated by red arrows, and other mutant alleles by black arrows. T, thrombospondin domain; Lg repeats, lagrin repeats; K, Kunitz domain; and Ig, immunoglobulin domain. A signal peptide is also present at the N terminus of each protein.

et al. 1999), where the *et4* and *sa580* mutations are located.

***mig-6* is present in pharyngeal basement membranes, but not expressed by pharyngeal cells:** We previously showed that *mig-6* transcripts are present in body-wall muscles, distal tip cells, and other unidentified cells and that the MIG-6 protein is present in body-wall muscles of embryos and then becomes enriched in the basement membranes of the pharynx, gonad, and intestine in larvae and adults (KAWANO *et al.* 2009). For this study, we re-examined the expression profile of a *mig-6::gfp* transcriptional reporter construct throughout embryonic and larval development and in adults with the aim of detecting possible pharyngeal expression. The following novel observations were made. During embryogenesis, the first expression is in the intestinal primordium followed at the comma and 1.5-fold stages by expression also in future head neurons and head muscle cells (Figure 4, A–C). Post-embryonic expression persists in head neurons and muscles, as well as in coelomocytes, body-wall muscles, anal depressor and sphincter, stomatointestinal muscle, and CAN neurons (Figure 4, D–G). Expression of the *mig-6::gfp* transcriptional reporter is never detected in pharyngeal cells at any stage during development or in adults. The MIG-6 protein that accumulates in the pharyngeal basement membrane (KAWANO *et al.* 2009) therefore likely originates from other cells, *e.g.*, from the body-wall muscle cells.

Overexpression of the metalloproteinase gene *mig-17* rescues the *mig-6(et4)* twisted pharynx phenotype: We previously showed that *mig-6* genetically interacts with *mig-17*, which encodes an ADAMTS protease, and that some *mig-6* mutant alleles cause MIG-17 protein to be abnormally distributed (KAWANO *et al.* 2009). To investigate if this could also be the case for the *mig-6(et4)* allele, we introduced a *mig-17::GFP* translational reporter construct where GFP is fused to the C-terminal end of the functional MIG-17 protein (NISHIWAKI *et al.* 2000) into a *mig-6(et4)* mutant background. No discernible changes in GFP distributions in the head or elsewhere in the body were observed, indicating that the *mig-6(et4)* allele does not cause dramatic changes in MIG-17 protein localization. To our surprise, we also

TABLE 1

Pharyngeal torsion angles in animals with various *mig-6* genotypes

Strains	Minimum angle(°)	Maximum angle (°)	Mean angle ± SEM(°)	*n*
Wild type				
N2	0	0	0	20
Homozygotes and heterozygotes of *mig-6(et4)* and *mig-6(sa580)*				
mig-6(et4)	17.9	43.3	28.9 ± 1.2	20
mig-6(sa580)	13.9	33.3	23.8 ± 1.2	20
mig-6(et4)/+	4.1	29	14 ± 1.2	20
mig-6(sa580)/+	2.3	18	8.3 ± 1.1	20
mig-6(et4)/mig-6(sa580)	12.4	32.6	21.9 ± 1.1	20
mig-6 alleles other than *et4* and *sa580*				
mig-6(k177)	0	0	0	20
mig-6(ev701)	0	0	0	20
mig-6(ev700)	0	0	0	20
mig-6(e1931)	0	0	0	20
mig-6(oz113)	0	0	0	20
mig-6(ev788)/eT1[a]	0	0	0	20
Rescue of *mig-6(sa580)* using cosmids ZK742 + C37C3				
Line 1, ZK742 + C37C3 in *mig-6(sa580)*	3.2	17.9	12.6 ± 1.0	17
Line 2, ZK742 + C37C3 in *mig-6(sa580)*	5.8	17.5	12.2 ± 1.3	11
Line 3, ZK742 + C37C3 in *mig-6(sa580)*	2.1	12.8	7.9 ± 0.6	25
Line 4, ZK742 + C37C3 in *mig-6(sa580)*	1.4	11.9	5.3 ± 0.6	27
Line 5, ZK742 + C37C3 in *mig-6(sa580)*	1.4	19.5	8.7 ± 1.9	11
Rescue of *mig-6(et4)* using minigenes *mig-6S* and *mig-6L*				
Line 1, pZH125 (*mig-6S*) in *mig-6(et4)*	0.1	16.1	3.8 ± 0.9	20
Line 2, pZH125 (*mig-6S*) in *mig-6(et4)*	0.1	23	8.2 ± 1.2	20
Line 3, pZH125 (*mig-6S*) in *mig-6(et4)*	0.9	25.5	8.1 ± 1.4	20
Line 4, pZH125 (*mig-6S*) in *mig-6(et4)*	0.2	25.5	6.3 ± 1.2	20
Line 1, pZH117 (*mig-6L*) in *mig-6(et4)*	0.0	29.5	11.9 ± 2.2	20
Line 2, pZH117 (*mig-6L*) in *mig-6(et4)*	2.2	28.1	14.1 ± 1.5	20
Rescue of *mig-6(sa580)* using minigenes *mig-6S* and *mig-6L*				
Line 1, pZH125 (*mig-6S*) in *mig-6(sa580)*	2.6	27.9	12.4 ± 1.9	20
Line 2, pZH125 (*mig-6S*) in *mig-6(sa580)*	0.9	25.9	11.2 ± 1.5	20
Line 1, pZH117 (*mig-6L*) in *mig-6(sa580)*	2.8	25.2	11.1 ± 1.9	11
Rescue of *mig-6(et4)* using a *mig-17::GFP* translational reporter				
Line 1, *mig-17::GFP* in N2	0	0	0	20
Line 1, *mig-17::GFP* in *mig-6(et4)*	5.2	21.7	12.5 ± 1.1	20
Phenocopies of *et4* and *sa580* phenotypes in wild-type N2				
Line 1, pQC10.1 (pZH125_*et4*) in N2	0.6	14.7	7.2 ± 1.0	20
Line 2, pQC10.1 (pZH125_*et4*) in N2	4.5	21.9	12.8 ± 1.3	15
Line 3, pQC10.1 (pZH125_*et4*) in N2	7.1	29	16.8 ± 1.7	15
Line 1, pQC10.2 (pZH125_*sa580*) in N2	2.9	17.7	10.8 ± 0.9	22

[a] *ev788* is a putative null allele, and homozygotes are lethal; *eT1* is used as a balancer.

observed that expression of the *mig-17::GFP* construct rescued pharynges in the *mig-6(et4)* mutant: the transgenic progeny had much straighter pharynges than the nontransgenic parental strain, with average twist angles of 12.5° ± 1.1° and 28.9° ± 1.2°, respectively (Figure 5 and Table 1). The same transgene introduced into wild-type worms did not produce any pharyngeal twist (Table 1). Overexpression of *mig-17* can therefore compensate for defects in *mig-6*, suggesting that the twisting force can be weakened by the proteolytic degradation of ECM components around the pharynx. Alternatively, MIG-17 activity could also lead to changes in the composition of the ECM that surrounds the pharynx, as occurs during distal tip cell migration where the MIG-17 protein helps recruit fibulin and nidogen to the gonadal ECM (Kubota *et al.* 2004, 2008).

Relationship between the Twp phenotype and ECM components/regulators: The fact that both *mig-6* and *mig-17* can influence the ECM to cause pharyngeal twist during growth led us to test other ECM components or regulators. The results are presented in Table 2, with representative images shown in Figure 6. Among ~20

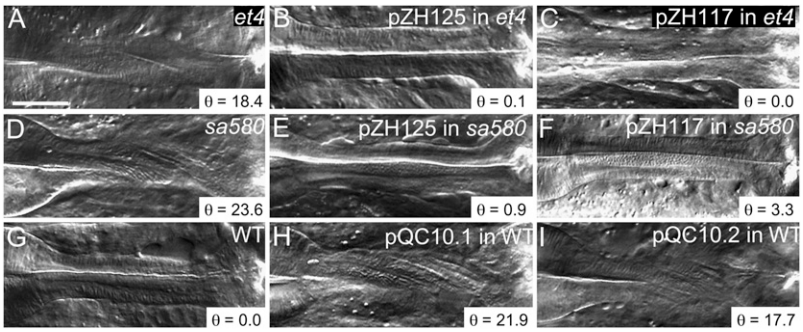

FIGURE 3.—Rescue and phenocopy of the *mig-6(et4)* and *mig-6(sa580)* twisted pharynges. (A-I) The pharynges of the indicated genotypes were photographed to emphasize the presence or absence of a pharyngeal twist in the isthmus. pZH125 is a plasmid bearing a *mig-6S* minigene, pZH117 is a plasmid bearing a *mig-6L* minigene, and pQC10.1 and pQC10.2 are modified versions of pZH125 in which the *et4* and *sa580* mutations, respectively, were introduced. Bar, 20 μm. The angle θ is that formed by the torsion lines and the anterior–posterior axis.

genes tested by RNAi, only three induced pharyngeal twists: *dig-1* (encodes a transmembrane protein with a large extracellular domain embedded in the ECM), *sax-7* (another gene encoding a transmembrane protein with a large extracellular domain), and *unc-52* (encodes perlecan).

Of the mutants examined, we found that three alleles of the gene *cle-1*, which encodes collagen XVIII, and three alleles of *dpy-7*, which encodes a cuticle collagen, produced the Twp phenotype (Table 2). All *cle-1* alleles that caused Twp represent partial deletions or late truncations of the amino acid sequence, and all of the *dpy-7* alleles that caused pharyngeal twists represent missense mutations that convert one amino acid to another. Two alleles of *lam-1*, which encodes laminin β, and one allele of *lam-3*, which encodes laminin α and γ, also produced the Twp phenotype. All the laminin mutations that cause twists introduce internal deletions. A nonsense mutation (*e444*) that introduces a stop codon at position 1811 of the perlecan protein encoded by *unc-52* also resulted in twisted pharynges. Several splice variants of perlecan are expressed from *unc-52*, with the longest isoform consisting of 3375 amino acids, and *e444* is not a null allele (ROGALSKI *et al.* 2001). Finally, mutations in the metalloproteinases *sup-17* and *adt-1* also caused pharyngeal twists.

Of all the mutants currently known to produce pharyngeal twists, only the *mig-6(et4)* and *mig-6(sa580)* alleles are 100% penetrant and always twist to the left (Table 2). RNAi against *unc-52*, *dig-1*, or *sax-7* caused the Twp phenotype with penetrances of 40–50% and produced a mixture of left- and right-handed pharyngeal twists (80%, 40%, and 26% of left-handed twisted pharynges, respectively). Similarly, specific mutations in some genes cause only left-handed pharyngeal twists, while others produced a mixture of left- or right-handed twists.

Genetic interactions with *mig-6(sa580)*: To explore possible epistatic interactions, we tested RNAi against ECM-related genes for their ability to reduce or increase the pharyngeal twist caused by the *mig-6(sa580)* allele (Table 3 and Figure 6). Of the ~20 genes tested, only RNAi against the genes *dpy-7*, *dig-1*, *fbl-1* (encodes fibulin), and *unc-52* reduced significantly and reproducibly the severity of the Twp phenotype in the *sa580* mutant background ($P < 0.05$). RNAi against some of the other genes tested occasionally inhibited the Twp phenotype of *sa580* mutants, as judged by the minimal twist angles observed, even if their mean torsion angle did not differ significantly from the *sa580* mutant. These were the genes *mig-17* and unc-71, encoding metalloproteinases, and *mig-23*, which encodes a nucleotide diphosphatase required for glycosylation and proper localization of MIG-17, as well as *lam-3*, which encodes laminin α and γ. The pharynx of *mig-6(sa580)* mutants combined with RNAi always twisted to the left irrespective of which RNAi was applied.

DISCUSSION

Mechanical basis of the pharyngeal twist (Twp phenotype): We have identified many genes that, when inhibited or mutated, can cause or inhibit the Twp phenotype in *C. elegans* (Table 4). These genes encode proteins related to the ECM either as intrinsic components (*e.g.*, collagens, laminins, fibulin, perlecan, papilin) or as ECM proteases of the ADAM and ADAMTS families (*e.g.*, ADT-1, MIG-17, SUP-17). A previous study had also identified mutant alleles of four other genes that caused pharyngeal twists: two encode transmembrane proteins with large extracellular domains (*dig-1* and *sax-7*) and one encodes a *C. elegans* septin (*unc-61*) (AXÄNG *et al.* 2007); the fourth, *mig-4*, remains unidentified. The nature of the mutations indicates that the Twp phenotype results from defects in the ECM or in ECM remodeling as the pharynx increases in size during larval growth. We showed previously that the radial contractile arrays within the pharyngeal muscle cells are bent within the twisted pharynges (AXÄNG *et al.* 2007). This is exactly what one would expect if these arrays elongated at their normal rate during larval growth but were constrained into bending by a recalcitrant ECM that is too rigid or otherwise flawed to expand appropriately. An over-rigid ECM can be expected if proteases responsible for its softening during growth are inhibited either by RNAi or genetic mutations or, if ECM components are mutated in such a way as to impair their malleability or regulation, by proteases or other factors. A general but limited model consistent with our results for some of the genes studied could be that

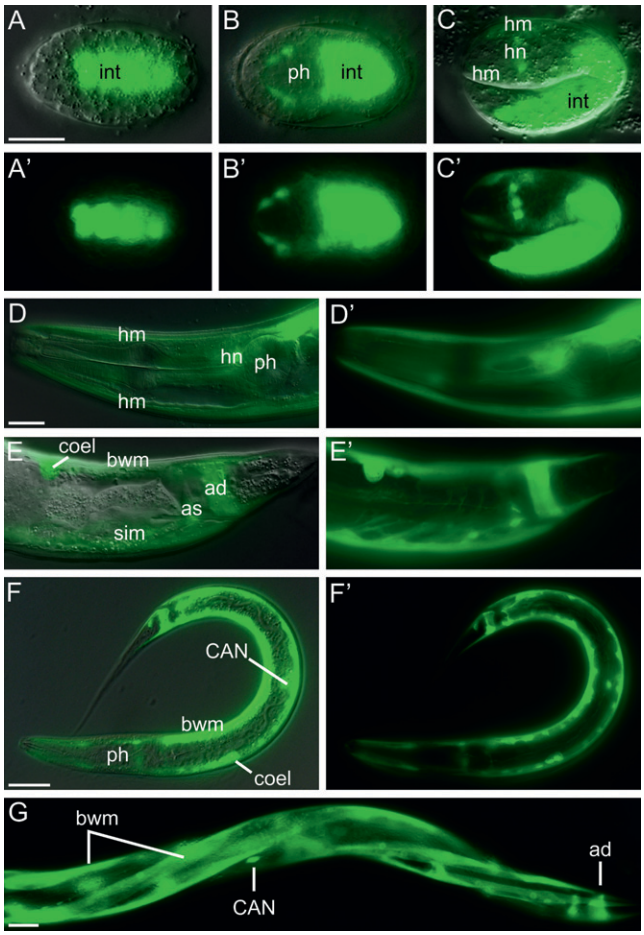

Figure 4.—Expression profile of a *mig-6* transcriptional GFP reporter. Worms transgenic for a *mig-6 promoter::gfp* construct were photographed under DIC illumination or epifluorescence using GFP filters. Each panel is provided as a DIC/GFP image overlay and as a GFP image alone, except for G, where only the GFP image is shown. The following developmental stages are shown: (A) an embryo at 270 min postfertilization at the E16 stage; (B) dorsal aspect of an embryo at the end of gastrulation, mid-plane; (C) 1.5-fold stage embryo; (D, E, and G) young adults; and (F) an L1 larva. int, intestine; ph, pharynx; hm, head muscle; hn, head neuron; bwm, body-wall muscle; coel, coelomocyte; ad, anal depressor; as, anal sphincter; sim, stomatointestinal muscle; CAN, CAN neuron. Each scale bar represents 20 μm; the bar in A applies to panels A through C while the bar in D applies to panels D and E.

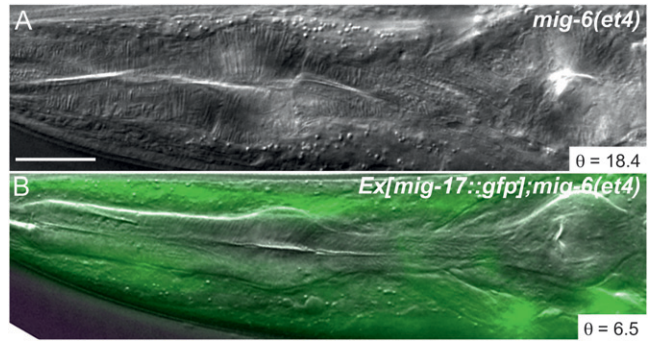

Figure 5.—*mig-17* rescues the Twp phenotype of *mig-6(et4)* mutants. (A) Twisted pharynx of a *mig-6(et4)* mutant and (B) straight pharynx of a *mig-6(et4)* worm rescued by a transgenic *mig-17::GFP* translational reporter construct. Bar, 20 μm. The angle θ is that formed by the torsion lines and the anterior–posterior axis.

MIG-6 and some metalloproteinases (*e.g.*, MIG-17) may promote softening of the ECM during growth, while other genes promote stiffening (*e.g.*, DIG-1 and FBL-1). This sort of model would explain why overexpressing *mig-17* or RNAi against *dig-1* and *fbl-1* can rescue Twp in the *mig-6(sa580)* mutant.

Most of the alleles so far identified to cause the Twp phenotype produce abnormal proteins, rather than being null alleles, and often cause a Twp phenotype that cannot be replicated by RNAi. For example, the *mig-6(et4)* and *mig-6(sa580)* alleles described here are missense mutations impacting the lagrin repeats of the MIG-6 protein. Specific functions for these domains have not been established, but they are likely involved in protein–protein interactions (Nardi *et al.* 1999; Kawano *et al.* 2009). Other *mig-6* alleles or RNAi against *mig-6* did not cause the Twp phenotype. Similarly, the three *dpy-7* alleles that cause Twp are missense mutations, while a fourth allele and RNAi caused no pharyngeal twist. The three *cle-1* alleles that cause Twp are either internal deletions or express a moderately truncated protein as is the case for *cle-1(cg120)*, while *cle-1* RNAi did not cause Twp. In the case of the metalloproteinases *adt-1* and *sup-17*, it is possible that the alleles that can cause a twisted pharynx phenotype have lost enzymatic activity. This is certainly true for the *adt-1(cn30)* allele, where the enzymatic domain is compromised by a deletion. Non-enzymatic effects of protease genes may relate to their ancillary domains that may sequester substrates, occupy binding sites within the ECM, or even compete with other proteases. Thus, it appears that the twisted pharynx is often the result of defective (as produced by the alleles of collagen, laminin, papilin, or perlecan that cause twists), depleted (as would result from some RNAi), or misregulated ECM components (as would result from the metalloproteinase mutations).

An intriguing observation relates to the semidominance of the *et4* and *sa580* alleles of *mig-6*, which appear to behave with near-precise additivity (Table 1), suggesting the possibility of a linear dose-dependent effect on the twist. Also intriguing was the fact that several alleles of *dpy-7*, which encodes a cuticle collagen, could cause the Twp phenotype. This suggests either that DPY-7 is present in the pharyngeal ECM or that defects in the cuticle lining the pharyngeal lumen (Albertson and Thomson 1976) may contribute to a Twp phenotype.

Another mechanistic consideration relates to the handedness of the pharyngeal twists: some mutations [*e.g.*, *mig-6(sa580)*, *cle-1(gk364)*, or *dpy-7(sc27)*] always produce left-handed twists, while other mutations produce mixtures of left- and right-handed twists [*e.g.*, *cle-*

TABLE 2

Genes that showed pharyngeal twist when mutated or depleted by RNAi in a wild-type background

Gene	Molecular identity	RNAi or allele	Mutation type	Minimum angle(°)	Maximum angle (°)	Mean angle ± SEM(°)	Twist incidence[a]	Twist direction[b]
N2 (wild type)	—	None		0	0	0	0%	—
adt-1	ADAMTS	*cn30*	Deletion, no enzymatic activity	0	14.9	2.2 ± 0.6	23%	78% left
adt-1	ADAMTS	RNAi		0	0	0	0	—
cle-1	Collagen XVIII	*cg120*	Deletion of exons 18–20, truncation	0	24.0	2.8 ± 0.8	30%	12% left
cle-1	Collagen XVIII	*gk364*	Internal deletion	0	22.4	2.6 ± 0.7	30%	0% left
cle-1	Collagen XVIII	*gk421*	Internal deletion	0	18.1	8.9 ± 0.7	95%	36% left
cle-1	Collagen XVIII	RNAi		0	0	0	0	—
dig-1	Adhesion molecule	RNAi		0	16.7	6.0 ± 1.5	45%	40% left
dpy-7	Cuticle collagen	*e1324*	Missense G189D	0	18.0	5.5 ± 1.0	50%	28% left
dpy-7	Cuticle collagen	*e88*	Missense G156R	0	21.4	8.6 ± 0.8	88%	20% left
dpy-7	Cuticle collagen	*sc27*	Missense G101R	0	18.4	5.1 ± 0.9	53%	0% left
dpy-7	Cuticle collagen	*m38*	Missense G201R	0	0	0	0	—
dpy-7	Cuticle collagen	RNAi		0	0	0	0	—
lam-1	Laminin β	*ok3139*	Internal deletion	0	20.6	3.7 ± 1.0	28%	0% left
lam-1	Laminin β	*ok3221*	Internal deletion	0	14.1	4.1 ± 0.8	43%	0% left
lam-3	Laminin α and γ	*ok2030*	Internal deletion	0	11.5	3.2 ± 0.6	60%	13% left
mig-6	Papilin	*et4*	Missense C973Y	17.9	43.3	28.9 ± 1.2	100%	100% left
mig-6	Papilin	*sa580*	Missense G965E	13.9	33.3	23.8 ± 1.0	100%	100% left
mig-6	Papilin	RNAi		0	0	0	0	—
sax-7	Adhesion molecule	RNAi		0	18.5	4.2 ± 1.2	50%	26% left
sup-17	ADAM	*n1258*	Missense V473D	0	13.3	1.0 ± 0.4	13%	0% left
sup-17	ADAM	*n1260*	Unknown	0	0	0	0	—
sup-17	ADAM	*n316*	Splicing mutant?	0	0	0	0	—
unc-52	Perlecan	*e444*	Truncated protein, V1811STOP	0	22.1	2.6 ± 0.8	33%	64% left
unc-52	Perlecan	RNAi		0	26.5	5.2 ± 1.7	40%	80% left

Only genes for which RNAi or at least one allele showed a significant effect ($P < 0.05$; *t*-test) are listed. Other genes examined by RNAi that showed no twist are the following: *adm-2*, *agr-1*, *dgn-1*, *gon-1*, *lam-3*, *mig-17*, *mig-23*, and *unc-71; emb-9*, *epi-1*, and *lam-1* RNAi were also tested but could not be scored due to lethality or sterility. Other mutant alleles that were examined but showed no twist are the following: *adm-2(ok3178)X*, *emb-9(g34)III*, *emb-9(b117)III*, *emb-9(b189)III*, *emb-9(g23)III*, *emb-9(hc70)III*, *epi-1(gm57)IV*, *fbl-1(k201)IV*, *fbl-1(k206)IV*, *gon-1 (e1254)/eDf18 IV*, *gon-1(q518) IV/nT1[unc(n754) let-?](IV;V)*, *let-2(b246)X*, *let-2(g25)X*, *let-2(g30)X*, *let-2(g37)X*, *mig-17(k113)V*, *mig-17(k174)V*, *mig-23(k180)X*, and *unc-71(e541)III*.

[a] Indicates what fraction of scored pharynges exhibited a twist. For RNAi, $n = 20$ in all cases, except *agr-1* ($n = 10$) and *adm-2* ($n = 9$); for mutants, $n = 40$ in all cases.

[b] Indicates the percentage of the twisted pharynges that twisted to the left; the others twisted to the right.

1(gk421), *dpy-7(e88)*, or *unc-52(e444)*]. Clearly, some alleles have an impact on the ordering of the molecules that make up the ECM such that a directional flaw is introduced while other alleles introduce no such bias. ECM molecules can also affect each other's ordering, as when COL-19 defects result in abnormal distribution of DPY-7 in the cuticle (Thein *et al.* 2003), which further complicates interpretations. Molecules known to organize themselves in ordered structures include laminins and collagens, for which we have now identified mutant alleles with twisted pharynges. In the future, it should be informative to determine how protein–protein interactions are altered in the mutant proteins that cause the Twp phenotype. Defects such as detachment and disorganization in the basement membrane surrounding the pharynx have already been documented for *dig-1* mutants by using electron microscopy (Bénard *et al.* 2006), and it will be interesting to examine the ultrastructure of other Twp mutants. It will also be valuable to examine double mutants among the genes that cause the Twp phenotype to establish genetic pathways.

Comparison with the Roller phenotype: The Twp phenotype is reminiscent of the Roller phenotype that results from missense or regulatory mutations, rather than from null mutations, in cuticular collagen genes. Kramer and Johnson (1993) carefully studied several alleles of the *sqt-1* (also known as *rol-5*) and *rol-6* genes, which encode subunits of a heterotrimeric collagen complex. As with the Twp phenotype, the Roller phenotype first appears at the L2 stage and worsens during growth. The *sqt-1* and *rol-6* genes are coordinately expressed during development (Park and Kramer 1994), and some mutant alleles cause left-handed Roller phenotypes, while others cause right-

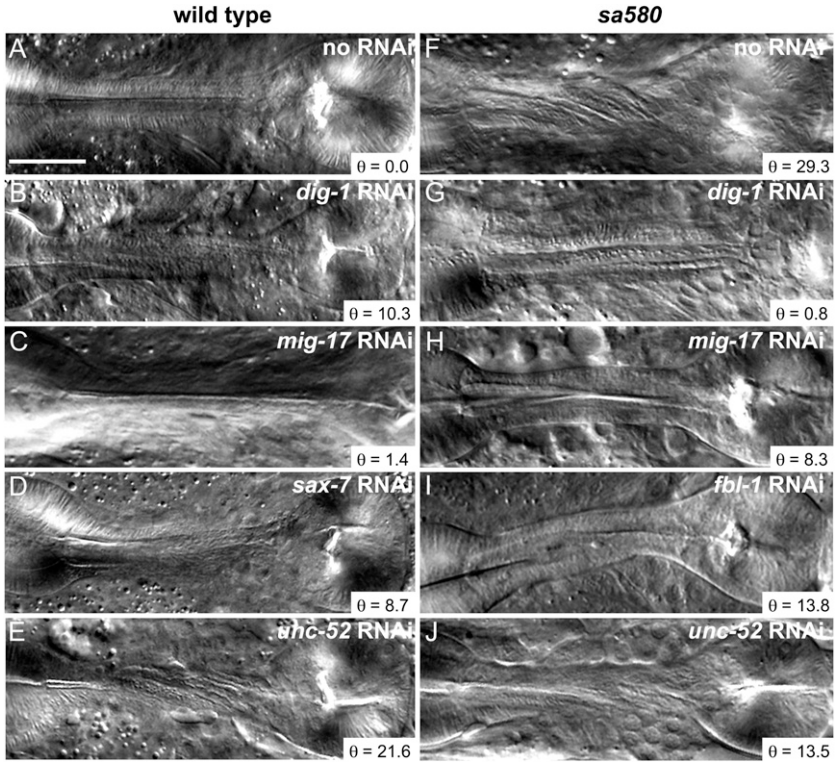

FIGURE 6.—RNAi knockdown of several genes affects the Twp phenotype. (A–E) The effects of RNAi against the indicated genes in wild-type N2 worms. (F–J) The effects of RNAi against the indicated genes in *mig-6(sa580)* mutant worms. Bar, 20 μm. The angle θ is that formed by the torsion lines and the anterior–posterior axis.

handed Roller phenotypes (KRAMER and JOHNSON 1993). The nature of the mutations, typically affecting conserved motifs implicated in disulfide bridges, suggests a model where too much or too little covalent interaction between subunits could cause cuticle alterations with opposite handedness. Ultrastructural analysis also helped provide a mechanical explanation for the Roller phenotype: a repetitive pentagonal pattern in the right-handed *rol-6(su1006)* mutant ectopically filled a space within the cuticle (PEIXOTO *et al.* 1998).

Why the pharynx? While the emphasis of this article is on the Twp phenotype, all of the genes studied here play important roles in other processes (see Table 4) ranging from maintenance of axon fasciculation [*e.g.*, *sax-7* (SASAKURA *et al.* 2005; WANG *et al.* 2005)], to distal tip cell migration [*e.g.*, *fbl-1* (KUBOTA *et al.* 2004), *mig-6* (KAWANO *et al.* 2009), *mig-17* (KUBOTA *et al.* 2008), and

TABLE 3

Effect of RNAi or overexpression of ECM-related genes on the pharyngeal twist caused by the *mig-6(sa580)* mutant allele

Gene	Molecular identity	RNAi/over expression	Mutant Background	Minimum angle (°)	Maximum angle (°)	Mean angle ± SEM (°)	Twist incidence[b]	Twist direction[c]
—	—	None	*mig-6(sa580)*	13.4	32.1	23.7 ± 1.0	100%	100% left
adt-1	ADAMTS	RNAi	*mig-6(sa580)*	17.0	34.4	26.2 ± 1.0	100%	100% left
cle-1	Collagen XVIII	RNAi	*mig-6(sa580)*	11.1	31.5	21.8 ± 1.4	100%	100% left
dig-1	Adhesion molecule	RNAi	*mig-6(sa580)*	0.8	13.8	5.3 ± 0.9[a]	100%	100% left
dpy-7	Cuticle collagen	RNAi	*mig-6(sa580)*	11.0	28.6	19.5 ± 1.1[a]	100%	100% left
fbl-1	Fibulin	RNAi	*mig-6(sa580)*	0.6	18.3	9.6 ± 1.0[a]	100%	100% left
lam-3	Laminin α and γ	RNAi	*mig-6(sa580)*	5.8	36.0	20.7 ± 1.0	100%	100% left
mig-17	ADAMTS	RNAi	*mig-6(sa580)*	5.9	33.1	21.4 ± 1.6	100%	100% left
mig-17::GFP	ADAMTS	Overexpression	*mig-6(et4)*	5.2	21.7	12.5 ± 1.1[a]	100%	100% left
mig-23	Nucleotide diphosphatase	RNAi	*mig-6(sa580)*	8.9	36.5	23.1 ± 1.6	100%	100% left
sax-7	Adhesion molecule	RNAi	*mig-6(sa580)*	12.0	41.2	25.1 ± 1.7	100%	100% left
unc-52	Perlecan	RNAi	*mig-6(sa580)*	6.0	28.4	19.4 ± 1.3[a]	100%	100% left
unc-71	ADAM	RNAi	*mig-6(sa580)*	4.7	32.3	20.8 ± 1.6	100%	100% left

[a] Indicates treatments that showed a significant difference in mean torsion angle compared to the reference strain *mig-6(sa580)* ($P < 0.05$; *t*-test). *lam-1* RNAi were tested but could not be scored due to lethality and sterility.

[b] Indicates what fraction of scored pharynges exhibited a twist. $n = 20$ in all cases.

[c] Indicates the percentage of twisted pharynges that twisted to the left; the others twisted to the right.

TABLE 4

Description of the genes that influenced the Twp phenotype

Gene	Protein type	Expression, function, and mutant phenotypes	References
adt-1	ADAMTS protease	Expressed in the head ganglion, ventral nerve cord, vulva, and rays of the male tail. The *cn30* allele lacking the protease activity exhibits defects in the formation of the male tail rays.	Kuno *et al.* (2002)
cle-1	Collagen type XVIII	Present at low levels in all basement membranes but enriched on neurons at synaptic contacts. The cg120 mutant lacks a terminal NC1/endostatin domain and exhibits cell migration and axon guidance defects as well as defective neuromuscular junctions. *gk364* and *gk421* are superficially wild type according to WormBase.	Ackley *et al.* (2001) Ackley *et al.* (2003)
dig-1	Large integral membrane protein	Expressed in muscles, hypodermal cells, and coelomocytes. Mutants exhibit defects in the maintenance of fasciculation and cell-body position, including defects in the positioning of several neurons and of the gonad primordium.	Bénard *et al.* (2006) Burket *et al.* (2006)
dpy-7	Cuticle collagen	Expressed by hypodermal cells and forms part of the cuticle that forms the exoskeleton. Mutants have abnormal body form and are typically short and fat.	Johnstone *et al.* (1992) Gilleard *et al.* (1997)
fbl-1	Fibulin	Expressed by head muscle cells and intestine, but accumulates on ECM of the pharynx, gonad, and other cells. The mutant exhibits enlarged gonads and has body-shape defects. FBL-1 antagonizes the ADAMTS protease GON-1 during gonad development, and its localization to ECM depends on MIG-17 activity.	Kubota *et al.* (2004) Hesselson *et al.* (2004) Kubota *et al.* (2008)
lam-1	Laminin β	Present in all ECM in *C. elegans*. Null mutants are lethal. RNAi treatment is also lethal, with embryos failing to properly separate various tissues and pharyngeal muscle cells separating into surrounding tissues.	Kao *et al.* (2006)
lam-3	Laminin α and γ	Present in all ECM in *C. elegans*. Null mutants are lethal, with missing or abnormal ECM and defective cell migration and differentiation.	C. C. Huang *et al.* (2003)
mig-6	Papilin	Transcript is expressed in distal tip cell, body-wall muscles, CAN neurons, and some other cells. Protein is enriched in the ECM of the pharynx, gonad, and intestine. Mutants fall into three allelic classes: *mig-6l* with defects in the longitudinal migration of the DTCs, *mig-6s* with defects in the second migration of the DTCs, and *mig-6Twp* that exhibit twisted pharynges (this study).	Kawano *et al.* (2009) This study
mig-17	ADAMTS protease	Transcript expressed by body-wall muscles. Protein accumulates on the basement membranes of gonad and pharynx and requires glycosylation for its recruitment to gonad surfaces. Its activity leads to the recruitment of nidogen to the ECM. Mutants have defects in some cell migrations, including DTC migration.	Nishiwaki *et al.* (2000) Kubota *et al.* (2004) Nishiwaki *et al.* (2004) Kubota *et al.* (2008) Kawano *et al.* (2009)
mig-23	Membrane-bound nucleoside diphosphatase	Expressed in the pharynx and intestine. It is required for glycosylation and proper localization of MIG-17. The mutant exhibits DTC migration defects similar to *mig-17* mutants.	Nishiwaki *et al.* (2004)

(*continued*)

TABLE 4

(Continued)

Gene	Protein type	Expression, function, and mutant phenotypes	References
sax-7	L1 CAM homolog	The protein is present in regions of cell–cell contacts during early embryogenesis and later in the nerve ring, nerve cord, pharynx, and gonad. It likely acts as a homo- and heterophilic adhesion molecule. Mutants have defects in blastomere compaction during gastrulation and exhibit embryonic lethality and abnormal neuronal distribution and trajectories.	Sasakura *et al.* (2005) Wang *et al.* (2005) Grana *et al.* (2010)
sup-17	ADAM proteinase orthologous to Drosophila and mouse KUZBANIAN	Activates signaling of NOTCH homolog LIN-12 by cleavage of the ectodomain. Mutants have defects in vulva development as well as in body morphology and male tail development; null alleles are embryonic lethal.	Jarriault and Greenwald (2005) Wen *et al.* (1997)
unc-52	Basement membrane heparan sulfate proteoglycan Perlecan	Three different isoforms (short, medium, and long) expressed differentially. All isoforms are expressed on muscle surfaces during embryogenesis, and, during late embryogenesis, the short form is enriched in the pharyngeal ECM while the medium form is enriched on body-wall muscles. Null mutants are lethal with defects in the formation of muscle filament lattices. Certain viable alleles have defects in distal tip cell migrations and/or defects in pharyngeal neuron development.	Rogalski *et al.* (1993) Mullen *et al.* (1999) Rogalski *et al.* (2001) Merz *et al.* (2003) Mörck *et al.* (2010)
unc-71	ADAM protease	Expressed by the excretory canal cell, the excretory gland, head neurons, and in epidermal cells of the vulva. The protein accumulates on membranes. Mutants have defects in motor axon guidance and sex myoblast migrations.	X. Huang *et al.* (2003)

DTC, distal tip cell

unc-52 (Merz *et al.* 2003)], or male tail morphogenesis [*e.g.*, *adt-1* (Kuno *et al.* 2002)], muscle development [*e.g.*, *unc-52* (Rogalski *et al.* 1993)], cuticle development [*e.g. dpy-7* (Johnstone *et al.* 1992)], and embryonic morphogenesis [*e.g.*, *lam-1* (Kao *et al.* 2006) and *lam-3* (C. C. Huang *et al.* 2003)]. However, mutations in these genes do not cause Roller or Squat phenotypes and share no other mutant phenotype in common in addition to Twp, although many also do exhibit cell migration defects, suggesting that both phenotypes are particularly sensitive to ECM remodeling defects. The pharynx is unique within the worm in the frequency and vigor with which it experiences muscular contractions at the pace of three to four pump cycles per second (Avery and Shtonda 2003), which probably also calls for special structural requirements that explain the thickness, 50–100 nm, of the basement membrane that surrounds it (C. C. Huang *et al.* 2003; Kramer 2005).

Future prospects: In humans, the sensitivity of muscle contraction to ECM defects probably explains why these are often implicated in congenital muscular dystrophies (Schessl *et al.* 2006). Similarly, there is a long list of genetic disorders, ranging from Marfan syndrome to deafness, myopathies and brain small-vessel disease, that have their roots in mutations that affect collagen genes, again drawing attention to the importance of ECM structure and regulation in human health (Carter and Raggio 2009). The sensitivity of the Twp phenotype to ECM defects represents a great opportunity to uncover, via forward genetics and with RNAi screens, many new genes and mechanisms important for ECM integrity and remodeling during organ growth. Such efforts will help elucidate the molecular mechanisms underlying ECM-related human diseases.

The *mig-17::GFP* fusion construct was a kind gift from K. Nishiwaki. The authors thank the technical assistance given by Avelino Javer in getting SHG images using the multimodal optical workstation at Institut de Ciències Fotòniques, Spain. This research was supported by grants from the following agencies: Vetenskapsrådet, Cancerfonden, Åhlén Stiftelse, Magnus Bergvalls Stiftelse, Carl Tryggers Stiftelse, and Erik Philip-Sörensens Stiftelse. J.G.C. also received grant support from the Canadian Institutes of Health Research (MOP-77722) and a Canada Research Chair (950-202224). M.A. was supported by a Howard Hughes Medical Institute Predoctoral Fellowship. Parts of this work were supported by a Public Health Service Grant to J.H.T. (R01 GM48700). M.M. thanks Generalitat de Catalunya, Spain, for an FI fellowship and a BE-Agaur-2008 fellowship, as well as the Sven and Lilly Lawski Foundation for a postdoctoral fellowship. Some

nematode strains used in this work were provided by the Caenorhabditis Genetics Center, which is funded by the National Insitutes of Health National Center for Research Resources.

LITERATURE CITED

Ackley, B. D., J. R. Crew, H. Elamaa, T. Pihlajaniemi, C. J. Kuo *et al.*, 2001 The NC1/Endostatin domain of *Caenorhabditis elegans* type XVIII collagen affects cell migration and axon guidance. J. Cell Biol. **152:** 1219–1232.

Ackley, B. D., S. H. Kang, J. R. Crew, C. Suh, Y. Jin *et al.*, 2003 The basement membrane components nidogen and type XVIII collagen regulate organization of neuromuscular junctions in *Caenorhabditis elegans*. J. Neurosci. **23:** 3577–3587.

Ailion, M., and J. H. Thomas, 2003 Isolation and characterization of high-temperature-induced Dauer formation mutants in *Caenorhabditis elegans*. Genetics **165:** 127–144.

Albertson, D. G., and J. N. Thomson, 1976 The pharynx of *Caenorhabditis elegans*. Philos. Trans. R. Soc. Lond. B Biol. Sci. **275:** 299–325.

Avery, L., and B. S. Shtonda, 2003 Food transport in the *C. elegans* pharynx. J. Exp. Biol. **206:** 2441–2457.

Axäng, C., M. Rauthan, D. H. Hall and M. Pilon, 2007 The twisted pharynx phenotype in *C. elegans*. BMC Dev. Biol. **7:** 61.

Bénard, C. Y., A. Boyanov, D. H. Hall and O. Hobert, 2006 DIG-1, a novel giant protein non-autonomously mediates maintenance of nervous system architecture. Development **133:** 3329–3340.

Brenner, S., 1974 The genetics of *Caenorhabditis elegans*. Genetics **77:** 71–94.

Burket, C. T., C. E. Higgins, L. C. Hull, P. M. Berninsone and E. F. Ryder, 2006 The *C. elegans* gene *dig-1* encodes a giant member of the immunoglobulin superfamily that promotes fasciculation of neuronal processes. Dev. Biol. **299:** 193–205.

Campbell, A. G., L. I. Fessler, T. Salo and J. H. Fessler, 1987 Papilin: a *Drosophila* proteoglycan-like sulfated glycoprotein from basement membranes. J. Biol. Chem. **262:** 17605–17612.

Carter, E. M., and C. L. Raggio, 2009 Genetic and orthopedic aspects of collagen disorders. Curr. Opin. Pediatr. **21:** 46–54.

Fessler, J. H., I. Kramerova, A. Kramerov, Y. Chen and L. I. Fessler, 2004 Papilin, a novel component of basement membranes, in relation to ADAMTS metalloproteases and ECM development. Int. J. Biochem. Cell Biol. **36:** 1079–1084.

Gaudet, J., and S. E. Mango, 2002 Regulation of organogenesis by the *Caenorhabditis elegans* FoxA protein PHA-4. Science **295:** 821–825.

Gilleard, J. S., J. D. Barry and I. L. Johnstone, 1997 cis regulatory requirements for hypodermal cell-specific expression of the *Caenorhabditis elegans* cuticle collagen gene *dpy-7*. Mol. Cell. Biol. **17:** 2301–2311.

Glasheen, B. M., R. M. Robbins, C. Piette, G. J. Beitel and A. Page-McCaw, 2010 A matrix metalloproteinase mediates airway remodeling in *Drosophila*. Dev. Biol. **344:** 772–783.

Grana, T. M., E. A. Cox, A. M. Lynch and J. Hardin, 2010 SAX-7/L1CAM and HMR-1/cadherin function redundantly in blastomere compaction and non-muscle myosin accumulation during *Caenorhabditis elegans* gastrulation. Dev. Biol. **344:** 731–744.

Hesselson, D., C. Newman, K. W. Kim and J. Kimble, 2004 GON-1 and fibulin have antagonistic roles in control of organ shape. Curr. Biol. **14:** 2005–2010.

Horner, M. A., S. Qhintin, M. E. Domeier, J. Kimble, M. Labouesse *et al.*, 1998 *pha-4*, an *HNF-3* homolog, specifies pharyngeal organ identity in *Caenorhabditis elegans*. Genes Dev. **12:** 1947–1952.

Huang, C. C., D. H. Hall, E. M. Hedgecock, G. Kao, V. Karantza *et al.*, 2003 Laminin alpha subunits and their role in *C. elegans* development. Development **130:** 3343–3358.

Huang, X., P. Huang, M. K. Robinson, M. J. Stern and Y. Jin, 2003 UNC-71, a disintegrin and metalloprotease (ADAM) protein, regulates motor axon guidance and sex myoblast migration in *C. elegans*. Development **130:** 3147–3161.

Jarriault, S., and I. Greenwald, 2005 Evidence for functional redundancy between *C. elegans* ADAM proteins SUP-17/Kuzbanian and ADM-4/TACE. Dev. Biol. **287:** 1–10.

Johnstone, I. L., Y. Shafi and J. D. Barry, 1992 Molecular analysis of mutations in the *Caenorhabditis elegans* collagen gene *dpy-7*. EMBO J. **11:** 3857–3863.

Kalb, J. M., K. K. Lau, B. Goszczynski, T. Fukushige, D. Moons *et al.*, 1998 *pha-4* is *Ce-fkh-1*, a *fork head*/HNF-3α, β, γ homolog that functions in organogenesis of the *C. elegans* pharynx. Development **125:** 2171–2180.

Kamath, R. S., M. Martinez-Campos, P. Zipperlen, A. G. Fraser and J. Ahringer, 2001 Effectiveness of specific RNA-mediated interference through ingested double-stranded RNA in Caenorhabditis elegans. Genome Biol. **2:** RESEARCH0002.

Kao, G., C. C. Huang, E. M. Hedgecock, D. H. Hall and W. G. Wadsworth, 2006 The role of the laminin beta subunit in laminin heterotrimer assembly and basement membrane function and development in *C. elegans*. Dev. Biol. **290:** 211–219.

Kawano, T., H. Zheng, D. C. Merz, Y. Kohara, K. K. Tamai *et al.*, 2009 *C. elegans mig-6* encodes papilin isoforms that affect distinct aspects of DTC migration, and interacts genetically with *mig-17* and collagen IV. Development **136:** 1433–1442.

Kramer, J. M., 2005 Basement membranes (September 1, 2005), *WormBook*, ed. The *C. elegans* Research Community, WormBook, doi/10.1895/wormbook.1.16.1, http://www.wormbook.org.

Kramer, J. M., and J. J. Johnson, 1993 Analysis of mutations in the *sqt-1* and *rol-6* collagen genes of *Caenorhabditis elegans*. Genetics **135:** 1035–1045.

Kramerova, I. A., N. Kawaguchi, L. I. Fessler, R. E. Nelson, Y. Chen *et al.*, 2000 Papilin in development; a pericellular protein with a homology to the ADAMTS metalloproteinases. Development **127:** 5475–5485.

Kramerova, I. A., A. A. Kramerov and J. H. Fessler, 2003 Alternative splicing of papilin and the diversity of *Drosophila* extracellular matrix during embryonic morphogenesis. Dev. Dyn. **226:** 634–642.

Kubota, Y., R. Kuroki and K. Nishiwaki, 2004 A fibulin-1 homolog interacts with an ADAM protease that controls cell migration in *C. elegans*. Curr. Biol. **14:** 2011–2018.

Kubota, Y., K. Ohkura, K. K. Tamai, K. Nagata and K. Nishiwaki, 2008 MIG-17/ADAMTS controls cell migration by recruiting nidogen to the basement membrane in *C. elegans*. Proc. Natl. Acad. Sci. USA **105:** 20804–20809.

Kuno, K., C. Baba, A. Asaka, C. Matsushima, K. Matsushima *et al.*, 2002 The *Caenorhabditis elegans* ADAMTS family gene adt-1 is necessary for morphogenesis of the male copulatory organs. J. Biol. Chem. **277:** 12228–12236.

Laprise, P., S. M. Paul, J. Boulanger, R. M. Robbins, G. J. Beitel *et al.*, 2010 Epithelial polarity proteins regulate *Drosophila* tracheal tube size in parallel to the luminal matrix pathway. Curr. Biol. **20:** 55–61.

Mango, S. E., E. J. Lambie and J. Kimble, 1994 The *pha-4* gene is required to generate the pharyngeal primordium of *Caenorhabditis elegans*. Development **120:** 3019–3031.

Mathew, M., S. I. Santos, D. Zalvidea and P. Loza-Alvarez, 2009 Multimodal optical workstation for simultaneous linear, nonlinear microscopy and nanomanipulation: upgrading a commercial confocal inverted microscope. Rev. Sci. Instrum. **80:** 073701.

Mello, C. C., J. M. Kramer, D. Stinchcomb and V. Ambros, 1991 Efficient gene transfer in *C. elegans*: extrachromosomal maintenance and integration of transforming sequences. EMBO J. **10:** 3959–3970.

Merz, D. C., G. Alves, T. Kawano, H. Zheng and J. G. Culotti, 2003 UNC-52/Perlecan affects gonadal leader cell migrations in *C. elegans* hermaphrodites through alterations in growth factor signaling. Dev. Biol. **256:** 173–186.

Miyabayashi, T., M. T. Palfreyman, A. E. Sluder, F. Slack and P. Sengupta, 1999 Expression and function of members of a divergent nuclear receptor family in *Caenorhabditis elegans*. Dev. Biol. **215:** 314–331.

Mörck, C., C. Axäng and M. Pilon, 2003 A genetic analysis of axon guidance in the *C. elegans* pharynx. Dev. Biol. **260:** 158–175.

Mörck, C., V. Vivekanand, G. Jafari and M. Pilon, 2010 *C. elegans ten-1* is synthetic lethal with mutations in cytoskeleton regulators, and enhances many axon guidance defective mutants. BMC Dev. Biol. **10:** 55.

Mullen, G. P., T. M. Rogalski, J. A. Bush, P. R. Gorji and D. G. Moerman, 1999 Complex patterns of alternative splicing mediate the spatial and temporal distribution of perlecan/UNC-52 in *Caenorhabditis elegans*. Mol. Biol. Cell **10:** 3205–3221.

Muriel, J. M., C. Dong, H. Hutter and B. E. Vogel, 2005 Fibulin-1C and fibulin-1D splice variants have distinct functions and assemble in a hemicentin-dependent manner. Development **132:** 4223–4234.

Nardi, J. B., R. Martos, K. K. Walden, D. J. Lampe and H. M. Robertson, 1999 Expression of lacunin, a large multidomain extracellular matrix protein, accompanies morphogenesis of epithelial monolayers in *Manduca sexta*. Insect Biochem. Mol. Biol. **29:** 883–897.

Nguyen, T. Q., H. Sawa, H. Okano and J. G. White, 2000 The *C. elegans* septin genes, *unc-59* and *unc-61*, are required for normal postembryonic cytokineses and morphogenesis but have no essential function in embryogenesis. J. Cell Sci. **113:** 3825–3837.

Nishiwaki, K., N. Hisamoto and K. Matsumoto, 2000 A metalloprotease disintegrin that controls cell migration in *Caenorhabditis elegans*. Science **288:** 2205–2208.

Nishiwaki, K., Y. Kubota, Y. Chigira, S. K. Roy, M. Suzuki *et al.*, 2004 An NDPase links ADAM protease glycosylation with organ morphogenesis in *C. elegans*. Nat. Cell Biol. **6:** 31–37.

Park, Y. S., and J. M. Kramer, 1994 The *C. elegans sqt-1* and *rol-6* collagen genes are coordinately expressed during development, but not at all stages that display mutant phenotypes. Dev. Biol. **163:** 112–124.

Peixoto, C. A., J. V. de Melo, J. M. Kramer and W. de Souza, 1998 Ultrastructural analyses of the *Caenorhabditis elegans rol-6 (su1006)* mutant, which produces abnormal cuticle collagen. J. Parasitol. **84:** 45–49.

Perkins, L. A., E. M. Hedgecock, J. N. Thomson and J. G. Culotti, 1986 Mutant sensory cilia in the nematode *Caenorhabditis elegans*. Dev. Biol. **117:** 456–487.

Portereiko, M. F., and S. E. Mango, 2001 Early morphogenesis of the *Caenorhabditis elegans* pharynx. Dev. Biol. **233:** 482–494.

Psilodimitrakopoulos, S., S. I. Santos, I. Amat-Roldan, A. K. Thayil, D. Artigas *et al.*, 2009 In vivo, pixel-resolution mapping of thick filaments' orientation in nonfibrilar muscle using polarization-sensitive second harmonic generation microscopy. J. Biomed. Opt. **14:** 014001.

Rogalski, T. M., B. D. Williams, G. P. Mullen and D. G. Moerman, 1993 Products of the unc-52 gene in *Caenorhabditis elegans* are homologous to the core protein of the mammalian basement membrane heparan sulfate proteoglycan. Genes Dev. **7:** 1471–1484.

Rogalski, T. M., G. P. Mullen, J. A. Bush, E. J. Gilchrist and D. G. Moerman, 2001 UNC-52/perlecan isoform diversity and function in *Caenorhabditis elegans*. Biochem. Soc. Trans. **29:** 171–176.

Rozario, T., and D. W. DeSimone, 2010 The extracellular matrix in development and morphogenesis: a dynamic view. Dev. Biol. **341:** 126–140.

Sasakura, H., H. Inada, A. Kuhara, E. Fusaoka, D. Takemoto *et al.*, 2005 Maintenance of neuronal positions in organized ganglia by SAX-7, a *Caenorhabditis elegans* homologue of L1. EMBO J. **24:** 1477–1488.

Schessl, J., Y. Zou and C. G. Bonnemann, 2006 Congenital muscular dystrophies and the extracellular matrix. Semin. Pediatr. Neurol. **13:** 80–89.

Starich, T. A., R. K. Herman, C. K. Kari, W. H. Yeh, W. S. Schackwitz *et al.*, 1995 Mutations affecting the chemosensory neurons of *Caenorhabditis elegans*. Genetics **139:** 171–188.

Sulston, J. E., and J. A. Hodgkin, 1988 Methods, pp. 587–606 in *The Nematode Caernorhabditis elegans*, edited by W. B. Wood. Cold Spring Harbor Laboratory Press, Cold Spring Harbor, NY.

Thein, M. C., G. McCormack, A. D. Winter, I. L. Johnstone, C. B. Shoemaker *et al.*, 2003 *Caenorhabditis elegans* exoskeleton collagen COL-19: an adult-specific marker for collagen modification and assembly, and the analysis of organismal morphology. Dev. Dyn. **226:** 523–539.

Tonning, A., J. Hemphala, E. Tang, U. Nannmark, C. Samakovlis *et al.*, 2005 A transient luminal chitinous matrix is required to model epithelial tube diameter in the *Drosophila* trachea. Dev. Cell **9:** 423–430.

Tsang, K. Y., M. C. Cheung, D. Chan and K. S. Cheah, 2010 The developmental roles of the extracellular matrix: beyond structure to regulation. Cell Tissue Res. **339:** 93–110.

Vogel, B. E., and E. M. Hedgecock, 2001 Hemicentin, a conserved extracellular member of the immunoglobulin superfamily, organizes epithelial and other cell attachments into oriented line-shaped junctions. Development **128:** 883–894.

Wang, X., J. Kweon, S. Larson and L. Chen, 2005 A role for the *C. elegans* L1CAM homologue *lad-1/sax-7* in maintaining tissue attachment. Dev. Biol. **284:** 273–291.

Wen, C., M. M. Metzstein and I. Greenwald, 1997 SUP-17, a *Caenorhabditis elegans* ADAM protein related to *Drosophila* KUZBANIAN, and its role in LIN-12/NOTCH signalling. Development **124:** 4759–4767.

Communicating editor: K. Kemphues

GENETICS

Supporting Information
http://www.genetics.org/cgi/content/full/genetics.110.120519/DC1

Genetics of Extracellular Matrix Remodeling During Organ Growth Using the *Caenorhabditis elegans* Pharynx Model

Gholamali Jafari, Jan Burghoorn, Takehiro Kawano, Manoj Mathew, Catarina Mörck, Claes Axäng, Michael Ailion, James H. Thomas, Joseph G. Culotti, Peter Swoboda and Marc Pilon

DOI: 10.1534/genetics.110.120519

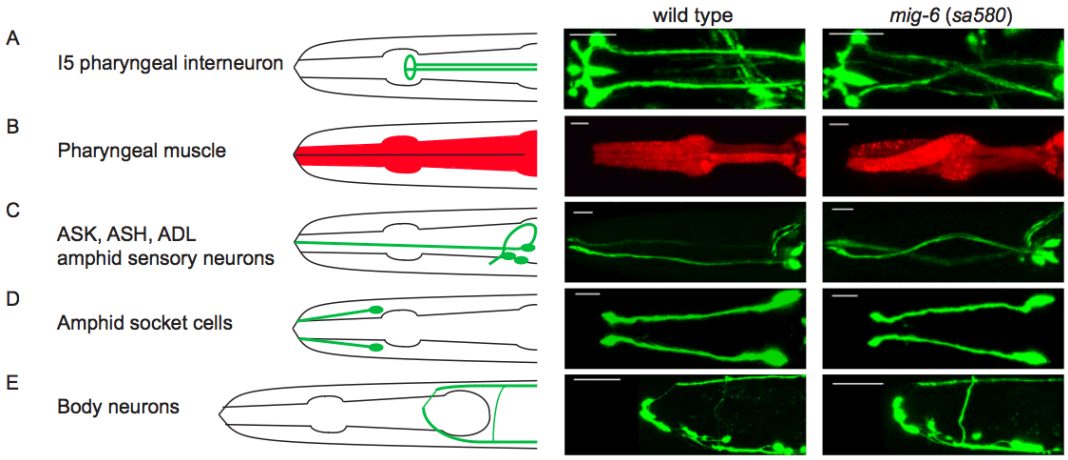

FIGURE S1.—Expression patterns or marker genes in different tissues in wild type (left) and mig-6 (sa580) (right). (A) I5 pharyngeal interneurons visualized by unc-53::gfp; (B) pharyngeal muscles visualized by myo-2::mCherry; (C) amphid sensory neurons ASK, ASH and ADL visualized by gpa-15::gfp; (D) amphid socket cells visualized by unc- 53::gfp; (E) body neurons visualized by unc-47::gfp. For this Figure, the transgenes unc-47::gfp (MCINTYRE et al. 1997), unc-53::gfp (STRINGHAM et al. 2002), and gpa-15::gfp (JANSEN et al. 1999) were introduced into the mig-6 (sa580) background by standard crossing. The transgene myo-2::mCherry (GAUDET and MANGO 2002) was introduced at 50 ng/μl into the mig-6 (sa580) background by standard germ line transformation (MELLO et al. 1991). All transgenic lines were maintained by using GFP or mCherry fluorescence as markers, and all transgenic lines were maintained as extrachromosomal arrays, with the exception of gpa-15::gfp, which was maintained as an integrated transgene. Images were acquired on a Zeiss Confocal Microscope LSM510 META and Zeiss software using a 40x objective. Worms were mounted on agarose pads and anaesthetized with 10 mM sodium azide.

References:

Gaudet, J., and S. E. Mango, 2002 Regulation of organogenesis by the Caenorhabditis elegans FoxA protein PHA- 4. Science 295: 821-825.

Jansen, G., K. L. Thijssen, P. Werner, M. van der Horst, E. Hazendonk et al., 1999 The complete family of genes encoding G proteins of Caenorhabditis elegans. Nat Genet 21: 414-419.

McIntire, S. L., R. J. Reimer, K. Schuske, R. H. Edwards and E. M. Jorgensen, 1997 Identification and characterization of the vesicular GABA transporter. Nature 389: 870-876.

Mello, C. C., J. M. Kramer, D. Stinchcomb and V. Ambros, 1991 Efficient gene transfer in C. elegans: extrachromosomal maintenance and integration of transforming sequences. EMBO J 10: 3959-3970.

Stringham, E., N. Pujol, J. Vandekerckhove and T. Bogaert, 2002 unc-53 controls longitudinal migration in C. elegans. Development 129: 3367-3379.